An entropy stable scheme for the multiclass Lighthill-Whitham-Richards traffic model

Raimund Bürger, Hector Torres,
Carlos A. Vega

PREPRINT 2018-38

SERIE DE PRE-PUBLICACIONES

An entropy stable scheme for the multiclass Lighthill-Whitham-Richards traffic model

Raimund Bürger[1], Héctor Torres[2] and Carlos A. Vega[3,*]

[1] *CI²MA and Departamento de Ingeniería Matemática, Facultad de Ciencias Físicas y Matemáticas, Universidad de Concepción, Casilla 160-C, Concepción, Chile*

[2] *Departamento de Matemáticas, Facultad de Ciencias, Universidad de La Serena, Av. Cisternas 1200, La Serena, Chile*

[3] *Departamento de Matemáticas y Estadística, División de Ciencias Básicas, Universidad del Norte, Barranquilla, Colombia*

Abstract. An entropy conservative (EC) numerical flux for the multiclass Lighthill-Whitham-Richards (MCLWR) kinematic traffic model based on the general framework by Tadmor [E. Tadmor, *The numerical viscosity of entropy stable schemes for systems of conservation laws, I*, Math. Comp., 49 (1987), pp. 91–103] is proposed. The approach exploits the existence of an entropy pair for a particular form of this model. The construction of EC fluxes is of interest since in combination with numerical diffusion terms they allow one to design entropy stable schemes for the MCLWR model. In order to obtain a higher-order accurate scheme and control oscillations near discontinuities, a third-order WENO reconstruction recently proposed by Ray [D. Ray, *Third-order entropy stable scheme for the compressible Euler equations*, in C. Klingenberg and M. Westdickenberg (eds.), Springer Proc. in Math. and Stat. 237, pp. 503–515] is used. Numerical experiments for different classes of drivers are presented to test the performance of the entropy stable scheme constructed with the entropy conservative flux proposed.

AMS subject classifications: Primary: 35L65. Secondary: 35L45, 765M06, 6T99, 90B20

Key words: multiclass Lighthill-Whitham-Richards traffic model, system of conservation laws, entropy conservative flux, entropy stable scheme

---

1 Introduction

The aim of this paper is to introduce an entropy conservative flux for the multiclass Lighthill-Whitham-Richards kinematic traffic model (MCLWR). This model is a generalization of the well-known Lighthill-Whitham-Richards model [18, 20] to multiple

*Corresponding author.

Email: rburger@ing-mat.udec.cl (Bürger), htorres@userena.cl (Torres), cvega@uninorte.edu.co (Vega)

classes of drivers and were independently formulated by Wong and Wong [28] and Benzoni-Gavage and Colombo [1]. The model is described by the nonlinear and spatially one-dimensional systems of conservation laws

$$\partial_t \boldsymbol{\rho} + \partial_x \boldsymbol{f}(\boldsymbol{\rho}) = 0, \quad (x,t) \in \mathbb{R} \times (0,\infty), \tag{1.1}$$

where $\boldsymbol{\rho} = \boldsymbol{\rho}(x,t) = (\rho_1,\dots,\rho_N)^{\mathrm{T}}$ is the vector of densities, that is, for each $i = 1,\dots,N$, ρ_i is the density of vehicles belonging to the class or species i, and $\boldsymbol{f}(\boldsymbol{\rho}) = (f_1(\boldsymbol{\rho}),\dots,f_N(\boldsymbol{\rho}))^{\mathrm{T}}$ is the flux vector. Under the assumptions that drivers of each class adjust their velocity to the total traffic density $\rho = \rho_1 + \dots + \rho_N$, and all drivers adjust their velocity in the same way, the MCLWR model is defined by the relationship

$$f_i(\boldsymbol{\rho}) = v_i^{\max} \rho_i \phi(\rho), \quad i = 1,\dots,N, \tag{1.2}$$

where $v_i^{\max}$ is the maximum velocity attained by cars in class i (free flowing speed) and $\phi(\rho)$ is a function describing the behavior of drivers. Some standard expressions for ϕ include the Greenshields model [14]

$$\phi(\rho) = 1 - \rho/\rho_{\max}, \tag{1.3}$$

where $\rho_{\max}$ is a maximum traffic density corresponding to the "bumper-to-bumper" situation, or the Drake model [7]

$$\phi(\rho) = \exp\left(-(\rho/\rho_0)^2/2\right). \tag{1.4}$$

It is further assumed that $0 < v_1^{\max} < \dots < v_N^{\max}$. Broad introductions to mathematical models for vehicular traffic, in particular on the choice of velocity functions within and the extensions of the LWR model, are provided in [12, 26, 27].

It is well known that the system (1.1), (1.2) is strictly hyperbolic in the interior of the phase space for (1.1),

$$\mathcal{D} := \{\boldsymbol{\rho} = (\rho_1,\dots,\rho_N)^{\mathrm{T}} \in \mathbb{R}^N : \rho_1 \geq 0,\dots,\rho_N \geq 0,\ \rho = \rho_1 + \dots + \rho_N \leq \rho_{\max}\},$$

and admits a separable entropy function (see below for detailed explanations) for arbitrary numbers N of driver classes, that is, of scalar equations in (1.1). The latter property is exceptional for systems of conservation laws of practical interest but does hold for the MCLWR models. On the other hand, it is a pre-requisite for the applicability of entropy stable schemes for systems of conservation laws that were proposed in a series of papers including [8–10, 23–25]. It is the purpose of this paper to demonstrate that entropy stable schemes, based on the use of an entropy conservative numerical flux, in combination with weighted essentially non-oscillatory (WENO) reconstructions indeed provide an accurate method for the numerical solution of the MCLWR model.

The hyperbolicity of the system (1.1), (1.2) has been studied by many authors. Benzoni-Gavage and Colombo [1] proved the hyperbolicity of the model by showing that the system is symmetrizable as long as $\rho_i > 0$ for all $i = 1, \ldots, N$. They constructed an explicit entropy pair (E, Q), that is, a convex function E which is termed the entropy function along with an associated entropy flux Q such that

$$\nabla_{\boldsymbol{\rho}} Q(\boldsymbol{\rho}) = \big(\partial_{\rho_1} Q(\boldsymbol{\rho}), \ldots, \partial_{\rho_N} Q(\boldsymbol{\rho})\big) = \boldsymbol{w}^{\mathrm{T}} \mathcal{J}_f(\boldsymbol{\rho}), \tag{1.5}$$

where

$$\boldsymbol{w} = \big(\partial_{\rho_1} E(\boldsymbol{\rho}), \ldots, \partial_{\rho_N} E(\boldsymbol{\rho})\big)^{\mathrm{T}} \tag{1.6}$$

is the vector of entropy variables. A system of conservation laws (1.1) endowed with an entropy pair satisfies the additional conservation law

$$\partial_t E(\boldsymbol{\rho}) + \partial_x Q(\boldsymbol{\rho}) = 0, \tag{1.7}$$

for smooth solutions of (1.1). We recall that for a given system (1.1), (1.1), the identity (1.5) represents N scalar equations for the two scalar functions E and Q, so for $N \geq 3$ the equality (1.5) is an overdetermined system of algebraic equations, and therefore the existence of an entropy pair (E, Q) satisfying (1.5) is an exceptional property.

It is well known that solutions of (1.1) develop discontinuities, therefore the entropy equation (1.7) transforms into the entropy inequality

$$\partial_t E(\boldsymbol{\rho}) + \partial_x Q(\boldsymbol{\rho}) \leq 0 \tag{1.8}$$

in the sense of distributions. There is interest in the design of conservative numerical schemes for (1.1), (1.2) that in semi-discrete (i.e., discrete in space but continuous in time) form satisfy an analogue of (1.8). Such entropy conservative (EC) schemes were introduced by Tadmor [22] and play an essential role in the construction of entropy stable schemes, since they can be used as a comparison principle to investigate entropy stability in the sense that a scheme that contains more numerical viscosity than an entropy conservative scheme is entropy stable (see [22], Theorem 5.2). The general framework introduced by Tadmor has been used in order to obtain entropy conservative schemes for some nonlinear systems of conservation laws, namely, the shallow water equations [10] and the Euler equations [15].

The remainder of this paper is organized as follows. In Section 2 we briefly review theory about entropy conservative schemes developed by Tadmor [22,23]. The computation of entropy conservative flux for the MCLWR traffic model (Greenshields form) is presented in Section 3. This section also contains a summary of the reconstruction procedure to obtained high order diffusion operators, in particular the third-order sign-preserving WENO method [11,19]. In Section 4 numerical experiments are provided. Finally, some conclusions are drawn in Section 5.

2 Entropy conservative schemes: general framework

2.1 Preliminaries

Let us consider a general one-dimensional system of conservation laws (1.1) independently of the context of the traffic model. Assume that there exists an entropy pair

(E,Q) associated with (1.1), then multiplying (1.1) by the entropy variables $\boldsymbol{w}^{\mathrm{T}} := \nabla_{\rho} E(\boldsymbol{\rho})$ yields that smooth solutions $\boldsymbol{\rho} = \boldsymbol{\rho}(x,t)$ satisfy (1.7). However, as is stated in Section 1, this identity is not valid for non-smooth solutions, therefore (1.7) transforms into the so-called entropy inequality (1.8) in the sense of distributions. A semi-discrete conservative and consistent scheme for (1.1) on a uniform spatial mesh $x_j = j\Delta x$, $j \in \mathbb{Z}$ is given by

$$\frac{\mathrm{d}\boldsymbol{\rho}_j(t)}{\mathrm{d}t} = -\frac{1}{\Delta x}\left(\boldsymbol{F}_{j+1/2} - \boldsymbol{F}_{j-1/2}\right), \quad j \in \mathbb{Z}, \tag{2.1}$$

where

$$\boldsymbol{\rho}_j(t) \approx \frac{1}{\Delta x}\int_{I_j} \boldsymbol{\rho}(\xi,t)\,\mathrm{d}t, \quad I_j := [x_{j-1/2}, x_{j+1/2}), \quad x_{j+1/2} := (j+1/2)\Delta x, \quad j \in \mathbb{Z},$$

and $\boldsymbol{F}_{j+1/2} = \boldsymbol{F}(\boldsymbol{\rho}_{j-p+1}, \dots, \boldsymbol{\rho}_{j+p})$ is the numerical flux associated with $x_{j+1/2}$. We assume that $\boldsymbol{F}_{j+1/2}$ is a Lipschitz continuous function and consistent with the differential flux in the standard sense, *i.e.* $\boldsymbol{F}(\boldsymbol{\rho}, \boldsymbol{\rho}, \dots, \boldsymbol{\rho}) = \boldsymbol{f}(\boldsymbol{\rho})$.

2.2 Entropy stable and entropy conservative numerical schemes

The scheme (2.1) is called *entropy stable* with respect to the entropy pair (E,Q) if it satisfies a discrete entropy inequality

$$\frac{\mathrm{d}}{\mathrm{d}t} E(\boldsymbol{\rho}_j(t)) + \frac{1}{\Delta x}\left(\tilde{Q}_{j+1/2} - \tilde{Q}_{j-1/2}\right) \leq 0 \tag{2.2}$$

for some *numerical entropy flux* $\tilde{Q}_{j+1/2}$ consistent with the entropy flux Q. If equality holds in (2.2), then the scheme (2.1) is called *entropy conservative*. Since inequality (2.2) holds for entropy stable schemes, such a scheme will be stable in an appropriate L^p space (see [8]).

Next we recall the basic result by Tadmor [22] related to the design of an entropy preserving numerical flux. First we introduce the notation

$$[\![a]\!]_{j+1/2} := a_{j+1} - a_j, \qquad \bar{a}_{j+1/2} := \frac{1}{2}(a_{j+1} + a_j).$$

Theorem 2.1 (Tadmor [22]). *Assume that the one-dimensional system of conservation laws* (1.1) *is endowed with an entropy pair* (E,Q). *Suppose that* $\tilde{\boldsymbol{F}}_{j+1/2}$ *is a consistent numerical flux that satisfies*

$$[\![\boldsymbol{w}]\!]_{j+1/2}^{\mathrm{T}} \tilde{\boldsymbol{F}}_{j+1/2} = [\![\psi]\!]_{j+1/2}, \quad j \in \mathbb{Z}, \tag{2.3}$$

where $\boldsymbol{w}^{\mathrm{T}} = \nabla_{\rho} E(\boldsymbol{\rho})$ *are the entropy variables and* ψ *is the so-called* entropy potential *defined by*

$$\psi(\boldsymbol{\rho}) := \boldsymbol{w}^{\mathrm{T}} \boldsymbol{f}(\boldsymbol{\rho}) - Q(\boldsymbol{\rho}). \tag{2.4}$$

Then the conservative scheme

$$\frac{\mathrm{d}\boldsymbol{\rho}_j(t)}{\mathrm{d}t} = -\frac{1}{\Delta x}\left(\tilde{\boldsymbol{F}}_{j+1/2} - \tilde{\boldsymbol{F}}_{j-1/2}\right), \quad j \in \mathbb{Z}, \tag{2.5}$$

is second-order accurate and entropy conservative, and satisfies the discrete entropy identity

$$\frac{\mathrm{d}}{\mathrm{d}t}E(\boldsymbol{\rho}_j(t)) = -\frac{1}{\Delta x}\left(\tilde{Q}_{j+1/2} - \tilde{Q}_{j-1/2}\right), \quad j \in \mathbb{Z}, \tag{2.6}$$

with the numerical entropy flux $\tilde{Q}_{j+1/2} = \bar{\boldsymbol{w}}^{\mathrm{T}}_{j+1/2}\tilde{\boldsymbol{F}}_{j+1/2} - \bar{\psi}_{j+1/2}$.

According to Theorem 2.1, the existence of an explicitly given entropy pair is an important ingredient in designing entropy conservative schemes. For the scalar case ($N = 1$), where any convex function can be used as an entropy function, the unique solution of (2.3) is given by [8]

$$\tilde{F}_{j+1/2} = \begin{cases} \dfrac{\psi_{j+1} - \psi_j}{w_{j+1} - w_j} & \text{if } \rho_j \neq \rho_{j+1}, \\ f(\rho_j) & \text{otherwise.} \end{cases} \tag{2.7}$$

For a system of conservation laws ($N > 1$), Tadmor proposed the following general solution of (2.3):

$$\tilde{\boldsymbol{F}}_{j+1/2} = \int_{-1/2}^{1/2} \boldsymbol{f}\big(\boldsymbol{w}_{j+1/2}(\xi)\big)\,\mathrm{d}\xi, \tag{2.8}$$

where $\boldsymbol{w}_{j+1/2}(\xi)$ denotes the straight line connecting $\boldsymbol{v}_j$ and $\boldsymbol{w}_{j+1}$, i.e.,

$$\boldsymbol{w}_{j+1/2}(\xi) = \frac{1}{2}(\boldsymbol{w}_j + \boldsymbol{w}_{j+1}) + \xi(\boldsymbol{w}_{j+1} - \boldsymbol{w}_j), \qquad \xi \in [-1/2, 1/2].$$

In general it is difficult to express the path integral (2.8) in closed form. However, this is feasible for MCLWR traffic flow models in the special case of $\phi(r)$ given by (1.3). In [23], Tadmor also constructed an explicit solution of (2.3) based on different paths in the phase space of the entropy variables. The procedure described by Tadmor is as follows: Let $\{\boldsymbol{r}_i\}_{i=1}^N$ be an arbitrary set of N linearly independent vectors, and let $\{\boldsymbol{l}_i\}_{i=1}^N$ be the corresponding orthogonal set. At an interface $x_{j+1/2}$, we define the paths

$$\boldsymbol{w}^0 := \boldsymbol{w}_j, \quad \boldsymbol{w}^i := \boldsymbol{w}^{i-1} + \left([\![\boldsymbol{w}]\!]^{\mathrm{T}}_{j+1/2}\boldsymbol{l}_i\right)\boldsymbol{r}_i \quad \text{for } i = 1, \dots, N-1, \quad \boldsymbol{w}^N := \boldsymbol{w}_{j+1}.$$

Then the entropy conservative flux is given by

$$\tilde{\boldsymbol{F}}_{j+1/2} = \sum_{i=1}^{N} \frac{\psi(\boldsymbol{w}^i) - \psi(\boldsymbol{w}^{i-1})}{[\![\boldsymbol{w}]\!]^{\mathrm{T}}_{j+1/2}\boldsymbol{l}_i}\,\boldsymbol{l}_i. \tag{2.9}$$

This algorithm has the disadvantage of increasing the computational cost due to the intensive use of of characteristic information. Besides, the computation of the flux (2.9) may be numerically unstable, as is pointed out in [10].

3 Entropy conservative numerical fluxes for traffic models

We start with a couple of simple examples for the scalar case.

Example 1. *For the Lighthill-Whitham-Richards (LWR) model along with the Greenshields relationship* (1.3)*, the traffic flow can be expressed as* $f(\rho) = v^{\max}\rho(1-\rho/\rho_{\max})$*. For the quadratic entropy* $E(\rho) = \rho^2/2$ *and the corresponding entropy flux*

$$Q(\rho) = v^{\max}\left(\frac{\rho^2}{3} - \frac{2\rho^3}{3\rho_{\max}}\right),$$

we obtain the entropy conservative flux

$$\tilde{F}_{j+1/2} = v^{\max}\left(\frac{\rho_{j+1}+\rho_j}{2} - \frac{\rho_{j+1}^2 + \rho_{j+1}\rho_j + \rho_j^2}{3\rho_{\max}}\right). \tag{3.1}$$

For the logarithmic entropy $E(\rho) = -\ln\rho$ *together with the corresponding entropy flux*

$$Q(\rho) = v^{\max}\left(\frac{2\rho}{\rho_{\max}} - \ln\rho\right),$$

the entropy variable and the entropy potential are $w = -1/\rho$ *and*

$$\psi(\rho) = v^{\max}\left(\ln\rho - \frac{\rho}{\rho_{\max}} - 1\right),$$

respectively. The resulting entropy conservative flux is

$$\tilde{F}_{j+1/2} = v^{\max}\rho_j\rho_{j+1}\left(\frac{1}{\rho_{j+1/2}^{\ln}} - \frac{1}{\rho_{\max}}\right). \tag{3.2}$$

Here, $a^{\ln}$ *is the logarithmic mean, defined as* $a_{j+1/2}^{\ln} := [\![a]\!]_{j+1/2}/[\![\ln(a)]\!]_{j+1/2}$*.*

Example 2. *For the Drake form of the traffic stream model* (1.4)*, the flux function takes the form* $f(\rho) = v^{\max}\rho\exp(-(\rho/\rho_0)^2/2)$*. The entropy potential in this case is* $\psi(\rho) = -v^{\max}\rho_0^2\exp(-(\rho/\rho_0)^2/2)$*. From* (2.7) *we obtain that the quadratic entropy* $E(\rho) = \rho^2/2$ *and the corresponding entropy flux*

$$Q(\rho) = v^{\max}\Big(\rho_0^2\exp\left(-(\rho/\rho_0)^2/2\right) + \rho^2\exp\left(-(\rho/\rho_0)^2/2\right)\Big)$$

result in the entropy conservative flux

$$\tilde{F}_{j+1/2} = \begin{cases} -v^{\max}\rho_0^2\dfrac{\exp\left(-(\rho_{j+1}/\rho_0)^2/2\right) - \exp\left(-(\rho_j/\rho_0)^2/2\right)}{\rho_{j+1}-\rho_j} & \text{if } \rho_j \neq \rho_{j+1}, \\ v^{\max}\rho_j\exp\left(-(\rho_j/\rho_0)^2/2\right) & \text{otherwise.} \end{cases} \tag{3.3}$$

3.1 Entropy conservative flux for a MCLWR traffic model

We now construct an entropy conservative flux for the MCLWR traffic model with the Greenshields speed-density relationship (1.3) based on the recipe (2.8). We begin with the entropy pair provided in [1], namely

$$E(\boldsymbol{\rho}) = \sum_{i=1}^{N} \frac{\rho_i(\ln \rho_i - 1)}{v_i^{\max}}, \quad Q(\boldsymbol{\rho}) = \phi(\rho) \sum_{i=1}^{N} \rho_i \ln \rho_i - \Phi(\rho),$$

where the function Φ is any primitive of ϕ, *i.e.*, $\Phi'(\rho) = V(\rho)$. According to (1.6), the corresponding entropy variables are

$$\boldsymbol{w} = \left(\frac{\ln \rho_1}{v_1^{\max}}, \dots, \frac{\ln \rho_N}{v_N^{\max}} \right)^{\mathrm{T}}, \tag{3.4}$$

and the entropy potential defined by (2.4) is

$$\psi(\rho) = \left(\frac{\ln \rho_1}{v_1^{\max}}, \dots, \frac{\ln \rho_n}{v_N^{\max}} \right) V(\rho) \begin{pmatrix} \rho_1 v_1^{\max} \\ \vdots \\ \rho_N v_N^{\max} \end{pmatrix} - V(\rho) \sum_{i=1}^{N} \rho_i \ln \rho_i + \Phi(\rho) = \Phi(\rho).$$

From (3.4) we obtain $\boldsymbol{\rho}(\boldsymbol{w}) = (\exp(v_1^{\max} w_1), \dots, \exp(v_N^{\max} w_N))^{\mathrm{T}}$. Then, for $V(\rho)$ given by (1.3), we get $\rho(\boldsymbol{w}) = \exp(v_1^{\max} w_1) + \dots + \exp(v_N^{\max} w_N)$, and we have

$$\boldsymbol{g}(\boldsymbol{w}) := \boldsymbol{f}(\boldsymbol{\rho}(\boldsymbol{w})) = \left(1 - \frac{1}{\rho_{\max}} \sum_{i=1}^{N} \exp\left(v_i^{\max} w_i\right) \right) \begin{pmatrix} v_1^{\max} \exp\left(v_1^{\max} w_1\right) \\ \vdots \\ v_N^{\max} \exp\left(v_N^{\max} w_N\right) \end{pmatrix}.$$

We denote by $\rho_{i,j}$ the density of class i on cell I_j, and fix the index j. Then the k-th component $g_k(\boldsymbol{w}_{j+1/2}(\xi))$ of the vector $\boldsymbol{g}(\boldsymbol{w}_{j+1/2}(\xi))$ can be written as

$$g_k(\boldsymbol{w}_{j+1/2}(\xi)) = \left(1 - \frac{1}{\rho_{\max}} \sum_{i=1}^{N} \exp(\alpha_i + \xi \beta_i) \right) v_k^{\max} \exp(\alpha_k + \xi \beta_k),$$

where $\alpha_i = v_i^{\max} \bar{w}_{i,j+1/2}$ and $\beta_i = v_i^{\max} [\![w_i]\!]_{j+1/2}$, or in terms of conserved variables,

$$\alpha_i = \ln \sqrt{\rho_{i,j} \rho_{i,j+1}} \quad \text{and} \quad \beta_i = \ln(\rho_{i,j+1} / \rho_{i,j}).$$

Thus, if $\beta_k \neq 0$, the numerical flux $\tilde{\boldsymbol{F}}_{j+1/2} = (\tilde{F}_{1,j+1/2}, \dots, \tilde{F}_{N,j+1/2})^{\mathrm{T}}$ is given by

$$\begin{aligned} \tilde{F}_{k,j+1/2} &= \int_{-1/2}^{1/2} g_k(\boldsymbol{w}_{j+1/2}(\xi)) \, \mathrm{d}\xi \\ &= \frac{v_k^{\max} \exp\left(\alpha_k\right)}{\beta_k} \left(\exp\left(\frac{\beta_k}{2}\right) - \exp\left(-\frac{\beta_k}{2}\right) \right) \end{aligned}$$

$$
\begin{aligned}
&- \frac{v_k^{\max}}{\rho_{\max}} \sum_{i=1}^{N} \frac{\exp\left(\alpha_i + \alpha_k\right)}{\beta_i + \beta_k} \left(\exp\left(\frac{\beta_i + \beta_k}{2} \right) - \exp\left(- \frac{\beta_i + \beta_k}{2} \right) \right) \qquad (3.5) \\
&= v_k^{\max} \left(\frac{\rho_{k,j+1} - \rho_{k,j}}{\ln(\rho_{k,j+1}) - \ln(\rho_{k,j})} - \frac{1}{\rho_{\max}} \sum_{i=1}^{N} \frac{\rho_{i,j+1}\rho_{k,j+1} - \rho_{i,j}\rho_{k,j}}{\ln(\rho_{i,j+1}\rho_{k,j+1}) - \ln(\rho_{i,j}\rho_{k,j})} \right) \\
&= v_k^{\max} \left((\rho_k)^{\ln}_{j+1/2} - \frac{v_k^{\max}}{\rho_{\max}} \sum_{i=1}^{N} (\rho_i \rho_k)^{\ln}_{j+1/2} \right).
\end{aligned}
$$

To elucidate that (3.5) defines a consistent numerical flux, it is sufficient to recall the well-known property

$$
\lim_{(\xi,\eta)\to(a_j,a_{j+1})} \frac{\xi - \eta}{\ln \xi - \ln \eta} = \begin{cases} 0, & \text{if } a_j = 0 \text{ or } a_{j+1} = 0, \\ a_j, & \text{if } a_j = a_{j+1}, \\ a^{\ln}_{j+1/2}, & \text{otherwise.} \end{cases}
$$

Thus, if we assume that $\boldsymbol{\rho}_{j+1/2} \to \boldsymbol{\rho} \in \mathcal{D}$ for all $j \in \mathbb{Z}$, we get, as expected,

$$
\tilde{F}_{k,j+1/2} \to v_k^{\max} \left(\rho_k - \frac{1}{\rho_{\max}} \sum_{i=1}^{N} \rho_i \rho_k \right) = v_k^{\max} \rho_k V(\rho).
$$

3.2 Higher-order entropy conservative fluxes

The entropy conservative fluxes described above are only second-order accurate. However, LeFloch, Mercier and Rohde [17] proposed a procedure to construct higher-order entropy conservative fluxes.The underlying idea is to consider linear combinations of existing second-order accurate entropy conservative fluxes $\tilde{\boldsymbol{F}}$.

Theorem 3.1 ([17], Th. 4.4). *For $p \in \mathbb{N}$, assume that $\gamma_1^p, \dots, \gamma_p^p$ solve the p linear equations*

$$
2 \sum_{r=1}^{p} r \gamma_r^p = 1, \qquad \sum_{r=1}^{p} r^{2s-1} \gamma_r^p = 1 \quad (s = 2, \dots, p),
$$

and define

$$
\tilde{\boldsymbol{F}}^{2p}_{j+1/2} := \sum_{r=1}^{p} \gamma_r^p \sum_{s=0}^{r-1} \tilde{\boldsymbol{F}}(\boldsymbol{\rho}_{j-s}, \boldsymbol{\rho}_{j-s+r}).
$$

Then the finite difference scheme with flux $\tilde{\boldsymbol{F}}^{2p}_{j+1/2}$ is $2p$-th order accurate for sufficiently smooth solutions $\boldsymbol{\rho}$ and entropy conservative, namely it satisfies the discrete entropy identity

$$
\frac{\mathrm{d}}{\mathrm{d}t} E\big(\boldsymbol{\rho}_j(t)\big) + \frac{1}{\Delta x} \big(\tilde{Q}^{2p}_{j+1/2} - \tilde{Q}^{2p}_{j-1/2} \big) \le 0,
$$

where the discrete entropy flux is given by

$$
\tilde{Q}^{2p}_{j+1/2} = \sum_{r=1}^{p} \gamma_r^p \sum_{s=0}^{r-1} \tilde{Q}(\boldsymbol{\rho}_{j-s}, \boldsymbol{\rho}_{j-s+r}). \qquad (3.6)
$$

For instance, the fourth-order entropy conservative flux corresponding to $p = 2$, namely $\tilde{\boldsymbol{F}}^4$ and which will be used in numerical examples, is given by

$$\tilde{\boldsymbol{F}}^4_{j+1/2} = \frac{4}{3}\tilde{\boldsymbol{F}}(\boldsymbol{\rho}_j, \boldsymbol{\rho}_{j+1}) - \frac{1}{6}\big(\tilde{\boldsymbol{F}}(\boldsymbol{\rho}_{j-1}, \boldsymbol{\rho}_{j+1}) + \tilde{\boldsymbol{F}}(\boldsymbol{\rho}_j, \boldsymbol{\rho}_{j+2})\big).$$

3.3 Additional numerical diffusion

Since the solutions of hyperbolic conservation laws develop discontinuities in finite time, the entropy conservative schemes lead to high-frequency oscillations in the vicinity of shocks (as was reported in [10, 24]). Therefore, it is necessary to add numerical diffusion to guarantee that entropy is dissipated. To this end, we used the higher-order numerical diffusion operator designed by Fjordholm et al [24]. In this reference, the numerical flux is defined as

$$\boldsymbol{f}_{j+1/2} = \tilde{\boldsymbol{F}}_{j+1/2} - \frac{1}{2}\boldsymbol{D}_{j+1/2}\langle\langle \boldsymbol{w}\rangle\rangle_{j+1/2}, \tag{3.7}$$

where $\tilde{\boldsymbol{F}}_{j+1/2}$ is a high-order entropy conservative flux, $\langle\langle \boldsymbol{w}\rangle\rangle_{j+1/2}$ is the difference in the reconstructed states, that is, $\langle\langle \boldsymbol{w}\rangle\rangle_{j+1/2} := \boldsymbol{w}_{j+1}(x_{j+1/2}) - \boldsymbol{w}_j(x_{j+1/2})$ for some reconstructed function $\boldsymbol{w}_j(x)$ which will be specified later, and $\boldsymbol{D}_{j+1/2}$ is a diffusion matrix of the form

$$\boldsymbol{D}_{j+1/2} = \boldsymbol{R}_{j+1/2}\boldsymbol{\Lambda}_{j+1/2}\boldsymbol{R}^{\mathrm{T}}_{j+1/2}. \tag{3.8}$$

Here, $\boldsymbol{R}_{j+1/2}$ is the matrix of right eigenvectors of the flux Jacobian $\mathcal{J}_f(\boldsymbol{\rho}_{j+1/2})$ and $\boldsymbol{\Lambda}_{j+1/2}$ is a positive diagonal matrix that depends on the eigenvalues of the flux Jacobian. In this work, we use the Rusanov-type diffusion term defined by

$$\boldsymbol{\Lambda}_{j+1/2} = \max\big\{|\lambda_1|, |\lambda_2|, \dots, |\lambda_N|\big\}\boldsymbol{I},$$

where $\lambda_1, \dots, \lambda_N$ are the eigenvalues of $\mathcal{J}_f(\boldsymbol{\rho}_{j+1/2})$ and $\boldsymbol{I}$ is the $N \times N$ identity matrix. The eigenvalues and the normalized eigenvectors are computed numerically by using the inexpensive framework based on the interlacing of known velocities with unknown eigenvalues [6].

In order to ensure entropy stability of the scheme with numerical flux (3.7), it is necessary to modify the reconstruction procedure and the following result will be extremely useful.

Lemma 3.1 (Fjordholm et al. [8]). *For each $j \in \mathbb{Z}$, let $\boldsymbol{D}_{j+1/2}$ given by* (3.8)*. Let $\boldsymbol{w}_j(x)$ be a polynomial reconstruction of the entropy variable in the cell I_j such that for each j, there exists a diagonal matrix $\boldsymbol{B}_{j+1/2} \geq 0$ such that*

$$\langle\langle \boldsymbol{w}\rangle\rangle_{j+1/2} = \big(\boldsymbol{R}^{\mathrm{T}}_{j+1/2}\big)^{-1}\boldsymbol{B}_{j+1/2}\boldsymbol{R}^{\mathrm{T}}_{j+1/2}[\![\boldsymbol{w}]\!]_{j+1/2} \tag{3.9}$$

Then the scheme with numerical flux (3.7) *is entropy stable with the following numerical entropy flux, where $\tilde{Q}^{2p}_{j+1/2}$ is defined by* (3.6)*:*

$$\hat{Q}_{j+1/2} = \tilde{Q}^{2p}_{j+1/2} - \frac{1}{2}\bar{\boldsymbol{w}}^{\mathrm{T}}\boldsymbol{D}_{j+1/2}\langle\langle \boldsymbol{w}\rangle\rangle_{j+1/2}.$$

As the authors of [8] pointed out, Lemma 3.1 provides sufficient conditions on the reconstruction for the scheme to be entropy stable. The last-mentioned reference also describes a reconstruction procedure that satisfies the crucial condition (3.9). This procedure can be summarized as follows. Assume that $\boldsymbol{w}_j$, $\boldsymbol{w}_{j+1}$, $\boldsymbol{w}_j^+$ and $\boldsymbol{w}_{j+1}^-$ are given. We then define the *scaled entropy variables*

$$\mathbf{z}_j^{\pm} := \boldsymbol{R}_{j\pm1/2}^{\mathrm{T}}\boldsymbol{w}_j, \qquad \tilde{\boldsymbol{z}}_j^{\pm} := \boldsymbol{R}_{j\pm1/2}^{\mathrm{T}}\boldsymbol{w}_j^{\pm} \tag{3.10}$$

Condition (3.9) can be expressed as

$$\langle\langle \tilde{\boldsymbol{w}} \rangle\rangle_{j+1/2} = \boldsymbol{B}_{j+1/2}\langle\langle \boldsymbol{w} \rangle\rangle_{j+1/2}. \tag{3.11}$$

We denote the l-th component of $\boldsymbol{z}_j$ and $\tilde{\boldsymbol{z}}_j$ by z_j^l and $\tilde{z}_j^l$, respectively. Then (3.11) is equivalent to the so-called *sign property* $\langle\langle \tilde{z}_j^l \rangle\rangle_{j+1/2} = \langle\langle z_j^l \rangle\rangle_{j+1/2}$. The reconstruction procedure of the scaled entropy variables that satisfy the sign property is carried out as follows (see [8, Corollary 3.5]). Given the interface values of each component $z = z^l$ of the scaled entropy variables $\boldsymbol{z}$ for a fix grid cell I_j, we define the point value $\mu_j^j := z_j^-$, and inductively

$$\mu_{s+1}^j := \mu_s^j + \delta_{s+1/2}, \quad s = j, j+1, \dots; \quad \mu_{s-1}^j := \mu_s^j - \delta_{s+1/2}, \quad s = j, j-1, \dots,$$

where $\delta_{s+1/2} = \langle\langle z \rangle\rangle_{s+1/2}$. Similarly, we define $\nu_j^j := z_j^+$ and

$$\nu_{s+1}^j := \nu_s^j + \delta_{s+1/2}, \quad s = j, j+1, \dots; \quad \nu_{s-1}^j := \nu_s^j - \delta_{s+1/2}, \quad s = j, j-1, \dots.$$

Let $\Upsilon_s^j(x) := \mathcal{R}_s(\{\mu_k^j\}_{k\in\mathbb{Z}})$ and $\Psi_s^j(x) := \mathcal{R}_s(\{\nu_k^j\}_{k\in\mathbb{Z}})$ be the reconstructions of μ^j and ν^j in cell I_s. Then the left and right reconstructed values are

$$\tilde{z}_j^- := \Upsilon_j^j(x_{j-1/2}) \quad \text{and} \quad \tilde{z}_j^+ := \Psi_j^j(x_{j+1/2})$$

Since (3.10) implies that $\boldsymbol{w}_j^{\pm} := (\boldsymbol{R}_{j\pm1/2}^{\mathrm{T}})^{-1}\tilde{\boldsymbol{z}}_j^{\pm}$, the diffusion term $\boldsymbol{D}_{j+1/2}\langle\langle \boldsymbol{w} \rangle\rangle_{j+1/2}$ can be expressed as

$$\begin{aligned}\boldsymbol{D}_{j+1/2}\langle\langle \boldsymbol{w} \rangle\rangle_{j+1/2} &= \boldsymbol{R}_{j+1/2}\boldsymbol{\Lambda}_{j+1/2}\boldsymbol{R}_{j+1/2}^{\mathrm{T}}\big(\boldsymbol{R}_{j+1/2}^{\mathrm{T}}\big)^{-1}\langle\langle \tilde{\boldsymbol{z}} \rangle\rangle_{j+1/2} \\ &= \boldsymbol{R}_{j+1/2}\boldsymbol{\Lambda}_{j+1/2}\langle\langle \tilde{\boldsymbol{z}} \rangle\rangle_{j+1/2}.\end{aligned}$$

It remains to specify the explicit reconstruction to be used in numerical experiments. It is well known that the ENO method satisfies the sign property [9] but the standard WENO methods fail to satisfy this property. However, Fjordholm and Ray [11] designed a third-order WENO reconstruction method (SP-WENO3 for short) that satisfies the sign property. Furthermore, the SP-WENO3 method has the advantage of leading to tighter stability bounds for higher-order accuracy compared to its ENO counterpart [11].

For the convenience of the reader, we briefly describe the SP-WENO3 method (see [11] for a complete description) for the scalar case (for one-dimensional systems, scaled entropy variables must be reconstructed as it is described above) by exhibiting the jump in reconstructed states. We denote the reconstructed values at the cell interfaces by $w^+_{j+1/2} = w_{j+1}(x_{j+1/2})$ and $w^-_{j+1/2} = w_j(x_{j+1/2})$. We also define the jump ratio at the interface $x_{j+1/2}$ as

$$\theta_j^- := \frac{[\![w]\!]_{j+1/2}}{[\![w]\!]_{j-1/2}} \quad \text{and} \quad \theta_j^+ := \frac{1}{\theta_j^-} = \frac{[\![w]\!]_{j-1/2}}{[\![w]\!]_{j+1/2}},$$

and the functions

$$\psi^+_{j+1/2} := \frac{1-\theta^-_{j+1}}{1-\theta^+_j}, \qquad \psi^-_{j+1/2} := \frac{1}{\psi^+_{j+1/2}}.$$

Then

$$\langle\!\langle w \rangle\!\rangle_{j+1/2} = \frac{1}{2}\big(\tilde{w}_0(1-\theta^-_{j+1}) + w_1(1-\theta_j^+)\big)[\![w]\!]_{j+1/2}, \tag{3.12}$$

with the weights given as $\tilde{w}_0 = 1/4 - 2C_2$ and $w_1 = 1/4 + 2C_1$. The functions C_1 and C_2 are chosen as

$$C_1(\theta_j^+, \theta^-_{j+1}) = \begin{cases} f^+/(8((f^+)^2 + (f^-)^2)) & \text{if } \theta_j^+ \neq 1, \psi^+ < 0, \psi^+ \neq -1, \\ 0 & \text{if } \theta_j^+ \neq 1, \psi^+ = -1, \\ -3/8 & \text{if } \theta_j^+ = 1 \text{ or } \psi^+ \geq 0, |\theta_j^+| \leq 1, \\ 1/8 & \text{if } \psi^+ \geq 0, |\theta_j^+| > 1, \end{cases}$$

and $C_2(\theta_j^+, \theta^-_{j+1}) = C_1(\theta^-_{j+1}, \theta_j^+)$, where

$$f^+(\theta_j^+, \theta^-_{j+1}) := \begin{cases} 1/(1+\psi^+) & \text{if } \theta_j^+ \neq 1, \psi^+ \neq -1 \\ 1 & \text{otherwise,} \end{cases} \qquad f^-(\theta_j^-, \theta^-_{j+1}) = f^+(\theta^-_{j+1}, \theta_j^+).$$

A modification of the SP-WENO reconstruction was recently proposed [19] in order to avoid the lack of numerical dissipation in regions where the solution has a convex or concave profile about the interface $x_{j+1/2}$. Such perturbation of the reconstruction procedure (3.12) preserves the sign property of the original method and gives better control of overshoots near discontinuities as it is reported in [19]. The modification consists on introducing a perturbation of (3.12) in the so-called C-region ($\theta_j^+ < 1$, $\theta^-_{j+1} > 1$ or $\theta_j^+ > 1$, $\theta^-_{j+1} < 1$), namely,

$$\langle\!\langle w \rangle\!\rangle_{j+1/2} = \frac{1}{2}\big(\tilde{w}_0(1-\theta^-_{j+1}) + w_1(1-\theta_j^+) + \mathcal{G}\big)[\![w]\!]_{j+1/2},$$

where

$$\mathcal{G} = \left(\min\left\{\frac{|[\![w]\!]_{j+1/2}|}{0.5(|w_j| + |w_{j+1}|)}, |[\![w]\!]_{j+1/2}|\right\}\right)^3.$$

Furthermore, it is necessary to modifify the WENO weights in C-region by taking

$$\widehat{C}_1 = \min\left\{\max\left\{\bar{C}_1, -\frac{3}{8}\right\}, \frac{1}{8}\right\}, \qquad \widehat{C}_2 = \min\left\{\max\left\{\bar{C}_2, -\frac{3}{8}\right\}, \frac{1}{8}\right\},$$

		$T = 0.01\,\mathrm{h}$				$T = 0.02\,\mathrm{h}$			
		EC-SP-WENO3		ENO3		EC-SP-WENO3		ENO3	
	M	L^1-err.	rate	L^1-err.	rate	L^1-err.	rate	L^1-err.	rate
Greenshields model	100	1.133	—	0.980	—	0.888	—	0.707	—
	200	0.604	0.907	0.515	0.927	0.440	1.012	0.351	1.009
	400	0.242	1.315	0.185	1.474	0.212	1.051	0.172	1.029
	800	0.113	1.104	0.087	1.079	0.108	0.972	0.092	0.891
	1600	0.068	0.731	0.058	0.581	0.054	0.998	0.045	1.040
Drake model	100	1.289	—	1.046	—	0.954	—	0.815	—
	200	0.577	1.158	0.457	1.196	0.396	1.267	0.316	1.367
	400	0.249	1.213	0.193	1.237	0.191	1.049	0.159	0.983
	800	0.117	1.085	0.096	1.013	0.093	1.040	0.076	1.067
	1600	0.054	1.120	0.044	1.116	0.051	0.850	0.036	1.062

Table 1: Example 1 (Greenshields and Drake models, $N = 1$): approximate L^1-errors and convergence rates.

where

$$\bar{C}_1 = C_1 - \frac{1}{4}\frac{\mathcal{G}}{(1-\theta_j^+)}, \qquad \bar{C}_2 = C_2 - \frac{1}{4}\frac{\mathcal{G}}{(1-\theta_{j+1}^-)}.$$

3.4 Time discretization

To solve (2.1) maintaining high order in time and simplicity, the explicit three-stage third-order *strong stability preserving* Runge-Kutta method SSPRK(3,3) will be used [13]. This method is given by the steps

$$\begin{aligned}
\boldsymbol{\rho}^{(1)} &= \boldsymbol{\rho}^n + \Delta t \boldsymbol{\mathcal{L}}(\boldsymbol{\rho}^n), \\
\boldsymbol{\rho}^{(2)} &= \frac{3}{4}\boldsymbol{\rho}^n + \frac{1}{4}\boldsymbol{\rho}^{(1)} + \frac{1}{4}\Delta t \boldsymbol{\mathcal{L}}(\boldsymbol{\rho}^{(1)}), \\
\boldsymbol{\rho}^{n+1} &= \frac{1}{3}\boldsymbol{\rho}^n + \frac{2}{3}\boldsymbol{\rho}^{(2)} + \frac{2}{3}\Delta t \boldsymbol{\mathcal{L}}(\boldsymbol{\rho}^{(2)}),
\end{aligned}$$

where

$$[\mathcal{L}(\boldsymbol{\Phi})]_j := -\frac{1}{\Delta x}\big(\boldsymbol{f}_{j+1/2} - \boldsymbol{f}_{j-1/2}\big).$$

To satisfy the CFL condition the value of Δt is computed adaptively for each step n. More exactly, the solution $\boldsymbol{\rho}^{n+1}$ at $t_{n+1} = t_n + \Delta t$ is calculated from $\boldsymbol{\Phi}^\nu$ by using the time step $\Delta t = \mathrm{CFL}\Delta x / \alpha^n_{\max}$, where $\alpha^n_{\max}$ is an estimate of the maximal characteristic velocity for $\boldsymbol{\rho}^n$. We take a CFL number of 0.4 throughout.

4 Numerical experiments

Numerical examples are conducted to show the performance (errors and graphics) of entropy stable fluxes developed along this work. Since exact solutions are not avail-

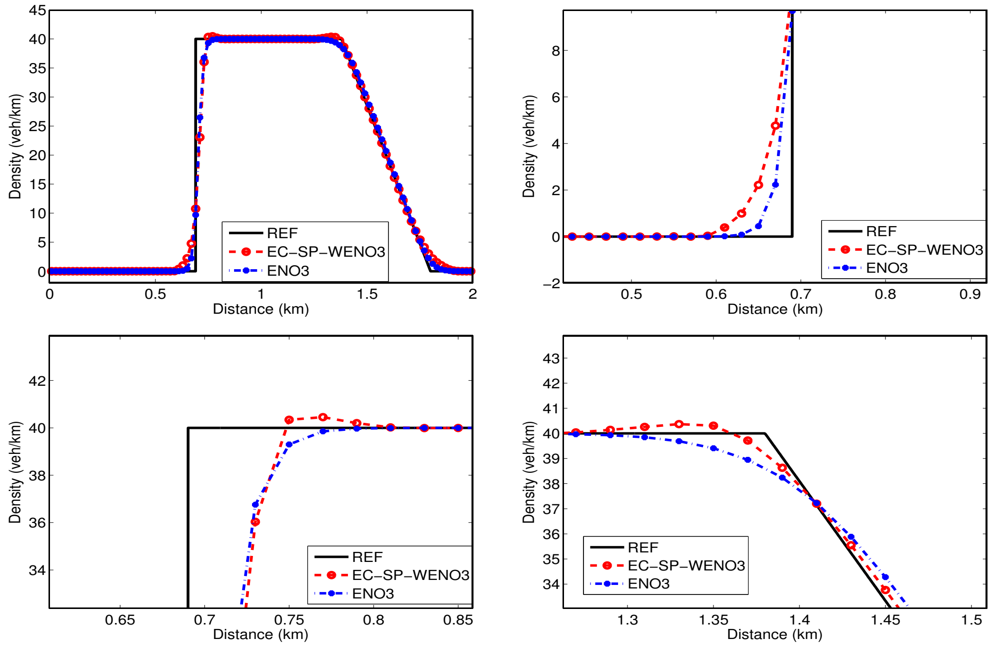

Figure 1: Example 1 (Greenshields model, $N = 1$): approximate solutions at $T = 0.01\,\mathrm{h}$ with $M = 100$ (top left) computed by EC-SP-WENO3c and ENO3, (top right and bottom) enlarged views.

able for $N \geq 2$ or complicated to construct, the errors for these cases are measured by using a reference solution. These approximate errors are computed as follows: let us denote by $\phi_i^N(\cdot, t)$ the numerical solution for the i-th component at time t calculated for the discretization $M \in \{100, 200, 400, 800, 1600\}$ and $\rho_i^{\mathrm{ref}}(\cdot, t)$ the corresponding reference solution, which is in all cases calculated by the widely used WENO5 component-wise method with $M = M_{\mathrm{ref}} = 6400$, and which is marked by "REF" in all plots. In all examples, numerical solutions obtained with entropy conservative flux obtained here along with the SP-WENO3c method (EC-SP-WENO3) are compared with the usual third-order ENO method (ENO3). Assume that $\rho_i^M(x, t) = \rho_{j,i}^M(t) = \text{const.}$ for $x \in I_j$; assume, moreover, that $\rho_i^{\mathrm{ref}}(\cdot, t)$ is piecewise constant on the mesh with meshwidth $1/M_{\mathrm{ref}}$. For a given time t and $r := M_{\mathrm{ref}}/M \in \mathbb{N}$ we then calculate the approximate L^1 error in species $i \in \{1, \dots, N\}$ by

$$e_i = e_i(t) = \left\| \rho_i^{\mathrm{ref}}(\cdot, t) - \rho_i^M(\cdot, t) \right\|_1 = \frac{1}{M_{\mathrm{ref}}} \sum_{j=0}^{M_{\mathrm{ref}}-1} \left| \rho_{j,i}^{\mathrm{ref}}(t) - \rho_{\lfloor j/r \rfloor, i}^M(t) \right|.$$

If we define $\rho_j^M(t) := \rho_{j,1}^M(t) + \cdots + \rho_{j,N}^M(t)$ (and analogously, $\rho_j^{\mathrm{ref}}(t)$), then the total approximate L^1 error at that time is given by

$$e_{\mathrm{tot}} = e_{\mathrm{tot}}(t) = \frac{1}{M_{\mathrm{ref}}} \sum_{j=0}^{M_{\mathrm{ref}}-1} \left| \rho_j^{\mathrm{ref}}(t) - \rho_{\lfloor j/r \rfloor}^M(t) \right|.$$

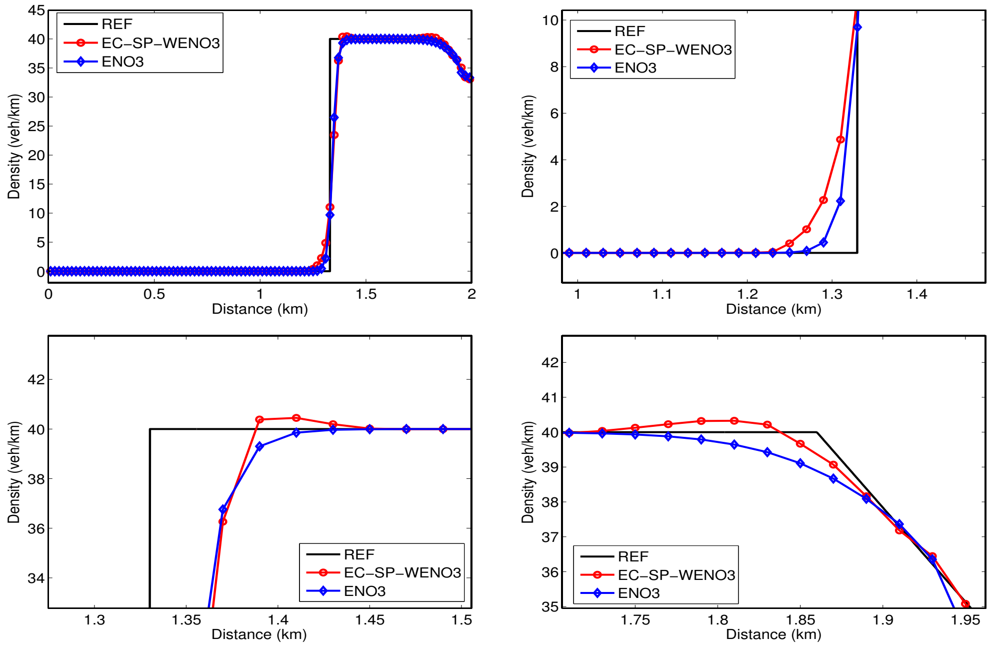

Figure 2: Example 1 (Greenshields model, $N = 1$): approximate solutions at $T = 0.02\,\mathrm{h}$ with $M = 100$ (top left) computed by EC-SP-WENO3c and ENO3, (top right and bottom) enlarged views.

In order to verify that the method is indeed entropy stable by displaying the relative change in total entropy for $t = t_n = n\Delta t$

$$\frac{\mathcal{E}(t_n) - \mathcal{E}(0)}{\mathcal{E}(0)}, \quad \text{where} \quad \mathcal{E}(t_n) := \Delta x \sum_{j=1}^{M} E\big(\boldsymbol{\rho}_j(t_n)\big). \tag{4.1}$$

Example 1 ($N = 1$)**.** *First, we test the entropy conservative fluxes* (3.1) *and* (3.3) *for the simple scalar case* ($N = 1$) *with data taken from [29]. Consider a highway of a length of* 2 km *with an initial platoon*

$$\rho(x,0) = 40\tau(x), \quad \text{where} \quad \tau(x) = \begin{cases} 10x & \text{if } 0 < x \leq 0.1, \\ 1 & \text{if } 0.1 < x \leq 0.9 \\ -10(x-1) & \text{if } 0.9 < x \leq 1, \\ 0 & \text{otherwise.} \end{cases} \tag{4.2}$$

The left boundary has no inflow ($\rho = 0$) for all time, and the right boundary is a free outflow. The free-flowing speed is $v^{\max} = 80\,\mathrm{km/h}$ and the jam density is $\rho_{\max} = 200\,\mathrm{veh/km}$.

For the Greenshields model, the numerical results at simulated final times $T = 0.01\,\mathrm{h}$ and $T = 0.02\,\mathrm{h}$ are displayed in Figures 1 and 2. The corresponding results for the Drake model are provided in Figures 3 and 4. Moreover, we display in Table 1 the approximate L^1-errors and convergence rates, and plot in Figure 5 the corresponding relative change in total entropy (4.1)*. In case of the Greenshields model, the breaking point $t_c = \rho_{\max}/800v^{\max}$ is depicted. This is the time at which the characteristics first intersect.*

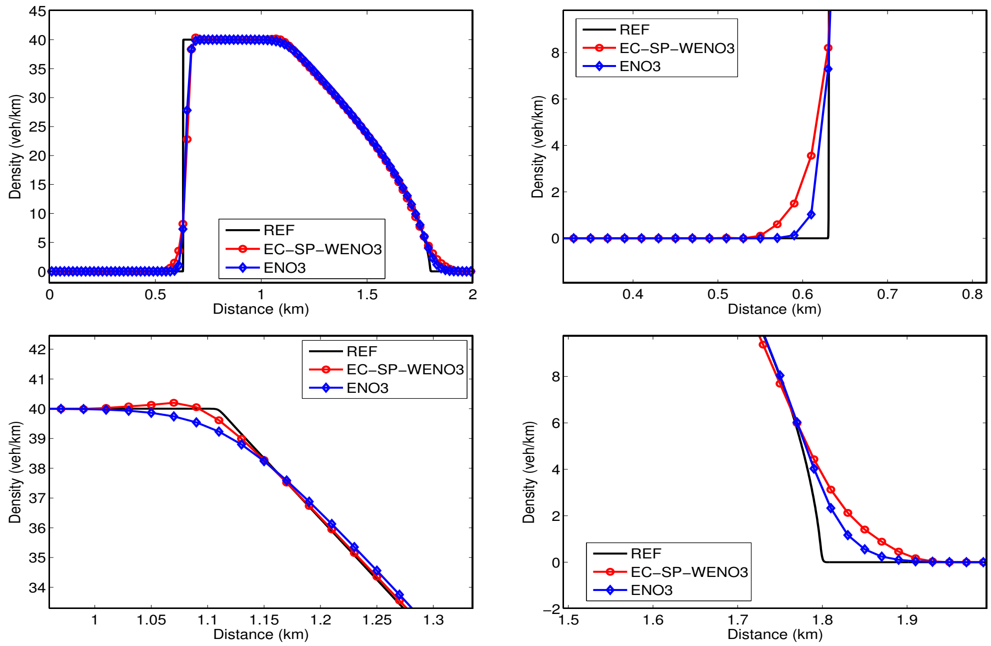

Figure 3: Example 1 (Drake model, $N = 1$): approximate solutions at $T = 0.01\,\mathrm{h}$ with $M = 100$ (top left) computed by EC-SP-WENO3c and ENO3, (top right and bottom) enlarged views.

Example 2 ($N = 2$)**.** *In order to test the performance of the entropy stable scheme developed here for systems, we consider the example proposed in [29] for $N = 2$ classes with the Greenshields model* (1.3)*. Consider a highway of a length of* $2\,\mathrm{km}$ *with an initial platoon* $\rho(x,0) = 40\tau(x)(0.5,0.5)^{\mathrm{T}}$*, where $\tau(x)$ is again given* (4.2)*. The left boundary has no inflow ($\rho_i = 0$) for all time, and the right boundary is a free outflow. The free-flowing driver speeds are* $v_1^{\max} = 60\,\mathrm{km/h}$ *and* $v_2^{\max} = \,\mathrm{km/h}$*, respectively. Equal distribution of drivers is assumed and the jam density is* $\rho_{\max} = 200\,\mathrm{veh/km}$.

Numerical results at $T = 0.01\,\mathrm{h}$ *and* $T = 0.015\,\mathrm{h}$ *are shown in Figures 6 and 7, respectively. The corresponding approximate L^1 errors are provided in Table 2, and the relative change in total entropy is shown in Figure 8. It is observed that the entropy conservative scheme proposed plus the dissipation term constructed from the SP-WENO approach control the oscillations near the discontinuities and reproduce the correct profile in smooth regions. Furthermore, the errors are comparable to those produced by the third-order ENO counterpart but with the advantage that entropy stability is ensured.*

Example 3 ($N = 9$)**.** *We now consider a scenario with $N = 9$ nine-class model proposed in [29], where the initial density distribution represents a platoon in the non-congested regime which is given by*

$$\rho(x,0) = 120\tau(x)(0.04, 0.08, 0.12, 0.16, 0.2, 0.16, 0.12, 0.08, 0.04)^{\mathrm{T}}. \qquad (4.3)$$

The free flowing speeds of drivers are taken as $v_i^{\max} = (52.5 + 7.5i)\,\mathrm{km/h}$, $i = 1,\dots,9$.

Numerical results at $T = 0.01\,\mathrm{h}$ *and* $T = 0.015\,\mathrm{h}$ *are shown in Figures 9 and 10, respectively. The corresponding approximate L^1 errors are provided in Table 3, and the relative*

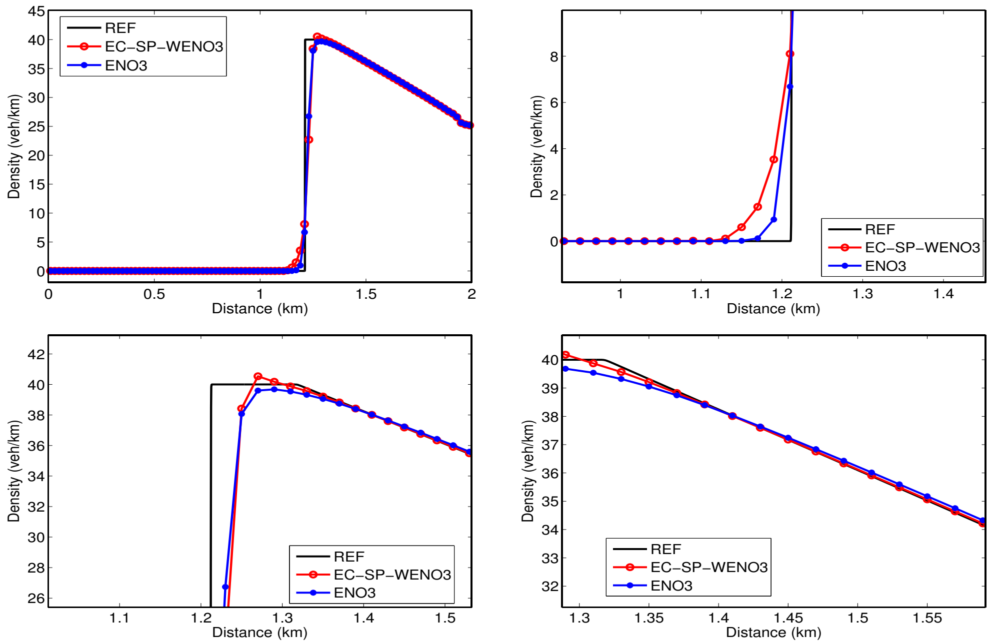

Figure 4: Example 1 (Drake model, $N = 1$): approximate solutions at $T = 0.02\,\mathrm{h}$ with $M = 100$ spatial gridpoints (top left) computed by EC-SP-WENO3 and ENO3, (top right and bottom) enlarged views.

change in total entropy is shown in Figure 11.

Example 4 ($N = 9$)**.** *Finally, we consider a circular road of length* $L = 4\,\mathrm{km}$ *with periodic boundary conditions*

$$\boldsymbol{\rho}(0,t) = \boldsymbol{\rho}(L,t), \quad t > 0. \tag{4.4}$$

The initial condition is the same as in Example 3, namely it is given by (4.3)*, where* $\tau(x)$ *is as in* (4.2)*.*

Numerical results at $T = 0.1\,\mathrm{h}$ *are shown in Figures 12, and the corresponding relative change in total entropy is shown in Figure 13. This demanding example illustrates the good behaviour of the entropy conservative flux proposed for approximating solutions that exhibit numerous discontinuities.*

5 Conclusions

The analysis and numerical examples in this contribution demonstrate that the particular structure of MCLWR models, in particular the existence of an entropy pair (E, Q), can sucessfully be exploited to construct entropy stable numerical schemes for the multiclass LWR traffic models given by (1.1), (1.2). In particular for some common examples of the function $\phi(\rho)$, namely those given by the Greenshields model (1.3), it is possible to obtain the entropy conservative flux in the systems case in closed algebraic form. Moreover, one may exploit the property of interlacing of the (in general,

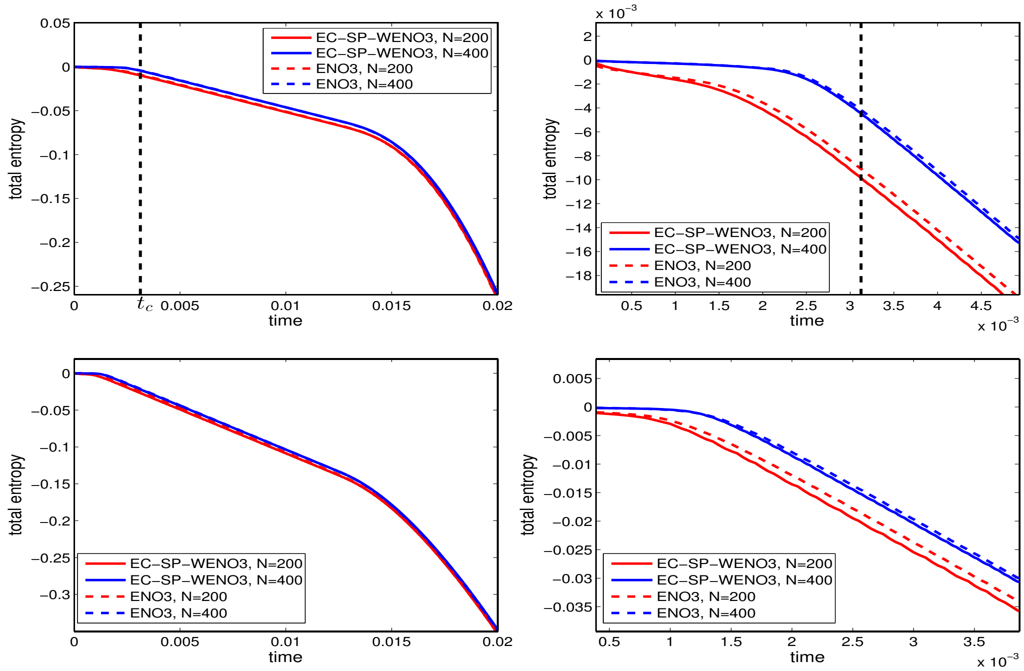

Figure 5: Example 1 (Greenshields model (top) and Drake model (bottom), $N = 1$): (left) relative change in total entropy of numerical solutions at two different mesh sizes, (right) enlarged view. For the Greenshield model, discontinuities appear after the critical time $t = t_c$ which can be computed explicitly.

unknown) eigenvalues of the flux Jacobian with the (known) velocities to define a Rusanov-type diffusion term that leads to an entropy stable scheme. In addition these properties permit to implement a sign-preserving WENO reconstruction [11].

Several extensions of the present treatment are conceivable. First of all, a closed-form representation of the entropy conservative flux similar to (3.5) can also be obtained for more general expressions than (1.3), for instance for $\phi(r) = (1 - r/\rho_{\max})^{\mathcal{N}}$ with $\mathcal{N} \in \mathbb{N}$. On the other hand, the system (1.1), (1.2) also describes phemomena different from traffic flows, for instance the settling of droplets and particles [4]. In the latter application (1.1) is posed on a finite vertical x-interval along with zero-flux boundary conditions. The application to settling as well as the MCLWR model may also be equipped with strongly degenerating diffusive corrections [5], so that the system (1.1) is replaced by the system of governing equations

$$\partial_t \boldsymbol{\rho} + \partial_x \boldsymbol{f}(\boldsymbol{\rho}) = \partial_x \big(\boldsymbol{B}(\boldsymbol{\rho})\partial_x \boldsymbol{\rho}\big), \tag{5.1}$$

where $\boldsymbol{B}(\boldsymbol{\rho})$ is an $N \times N$ positive semidefinite, possibly degenerating diffusion matrix, posed along with initial conditions and possibly periodic or zero-flux boundary conditions. It is possible to formulate entropy conservative methods also for convection-diffusion systems of this type [16] provided that the first-order system (1.1) possesses an entropy pair and moreover the flux Jacobian $\mathcal{J}_f(\boldsymbol{\rho})$ and $\boldsymbol{B}(\boldsymbol{\rho})$ have the same eigenvectors. For practically all models of interest, the latter condition is only satisfied when $\boldsymbol{B}(\boldsymbol{\rho})$ is a multiple of the $N \times N$ identity matrix [3].

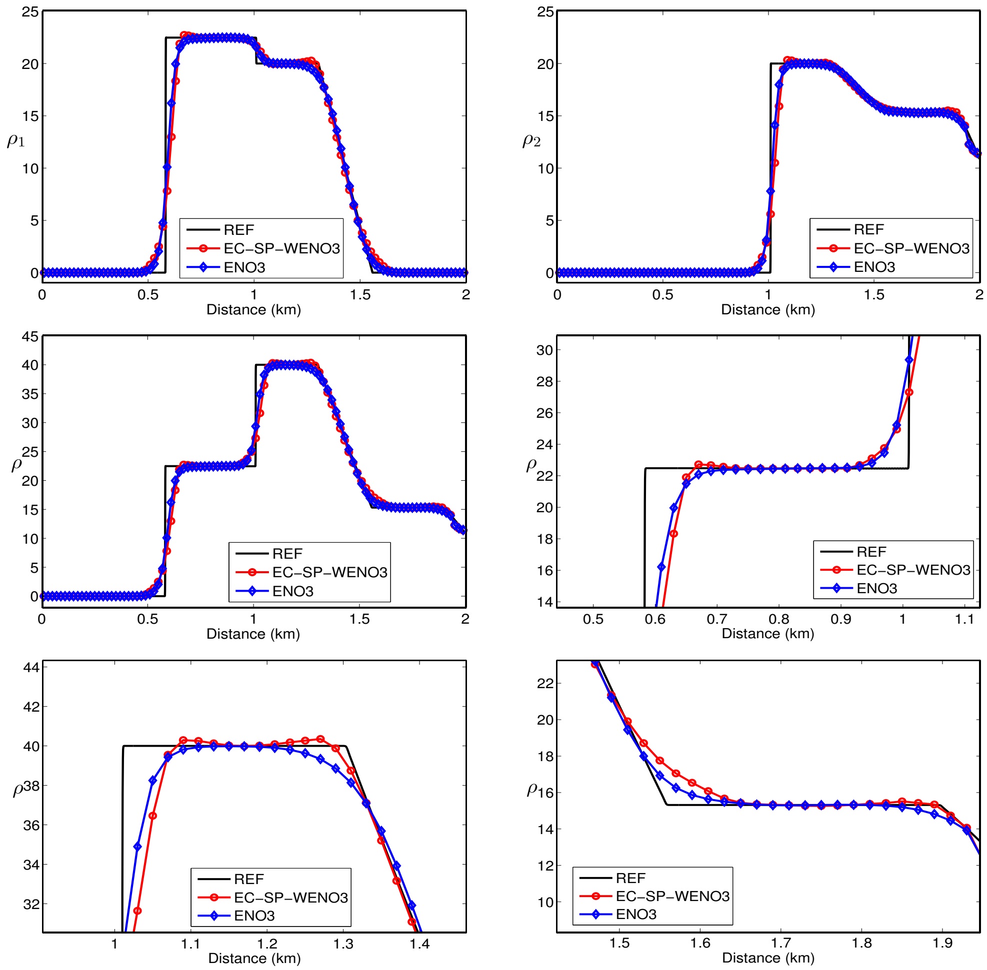

Figure 6: Example 2 (Greenshields model, $N = 2$): approximate solutions at $T = 0.01\,\mathrm{h}$ with $M = 100$ spatial cells corresponding to (top left) class 1, (top right) class 2, (middle left) the total density, and (middle right and bottom) enlarged views of the total density.

Acknowledgements

RB is acknowledges support by Fondecyt project 1170473; CONICYT/PIA/Concurso Apoyo a Centros Científicos y Tecnológicos de Excelencia con Financiamiento Basal AFB170001; and CRHIAM, project CONICYT/FONDAP/15130015. HT is supported by by the Dirección de Investigación y Desarrollo of Universidad de La Serena through DIDULS project PR17151. CV acknowledges support by Fundación para la Promoción de la Investigación y la Tecnología (FPIT) del Banco de la República.

References

[1] S. Benzoni-Gavage and R.M. Colombo, *An n-populations model for traffic flow*, Eur. J.

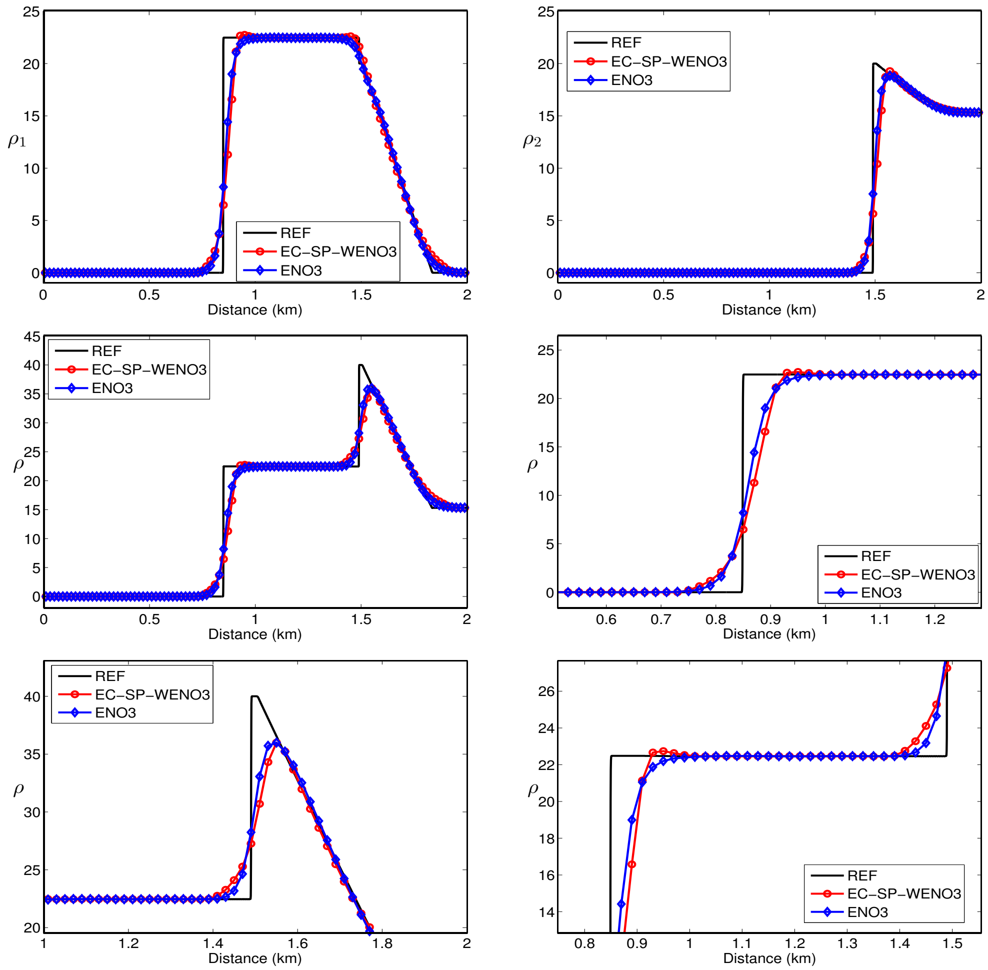

Figure 7: Example 2 (Greenshields model, $N = 2$): approximate solutions at $T = 0.015\,\mathrm{h}$ with $M = 100$ spatial cells corresponding to (top left) class 1, (top right) class 2, (middle left) the total density, and (middle right and bottom) enlarged views of the total density.

Appl. Math., 14 (2003), pp. 587–612.

[2] S. Benzoni-Gavage, R.M. Colombo, and P. Gwiazda, *Measure valued solutions to conservation laws motivated by traffic modelling*, Proc. Roy. Soc. A, 462 (2006), pp. 1791–1803.

[3] R. Bürger, P.E. Méndez, and C. Parés, *On entropy stable schemes for degenerate parabolic multispecies kinematic flow models*. Preprint 2018-24, Centro de Investigación en Ingeniería Matemática, Universidad de Concepción; submitted.

[4] R. Bürger, P. Mulet, and L. Rubio, *Implicit-explicit methods for the efficient simulation of the settling of dispersions of droplets and colloidal particles*, Adv. Appl. Math. Mech., 10 (2018), pp. 445–467.

[5] R. Bürger, P. Mulet, and L.M. Villada, *A diffusively corrected multiclass Lighthill-Whitham-Richards traffic model with anticipation lengths and reaction times*, Adv. Appl. Math. Mech., 5 (2013), pp. 728–758.

[6] R. Donat and P. Mulet, *Characteristic-based schemes for multi-class Lighthill-Whitham-Richards traffic models*, J. Sci. Comput., 37 (2008), pp. 233–250.

		EC-SP-WENO3				ENO3			
		ρ_1		ρ_2		ρ_1		ρ_2	
	M	L^1-err.	rate	L^1-err.	rate	L^1-err.	rate	L^1-err.	rate
$T = 0.01\,\mathrm{h}$	100	1.052	—	0.710	—	0.878	—	0.583	—
	200	0.483	1.123	0.318	1.160	0.442	0.989	0.279	1.064
	400	0.226	1.094	0.150	1.079	0.210	1.075	0.132	1.072
	800	0.101	1.167	0.065	1.199	0.093	1.162	0.058	1.179
	1600	0.046	1.125	0.029	1.162	0.043	1.121	0.026	1.150
$T = 0.015\,\mathrm{h}$	100	1.017	—	0.637	—	0.861	—	0.507	—
	200	0.459	1.148	0.290	1.132	0.414	1.055	0.248	1.031
	400	0.221	1.054	0.137	1.077	0.200	1.047	0.118	1.066
	800	0.101	1.118	0.060	1.184	0.095	1.075	0.053	1.145
	1600	0.047	1.106	0.028	1.086	0.043	1.119	0.024	1.131

Table 2: Example 2 (Greenshields model, $N = 2$): approximate L^1-errors and convergence rates.

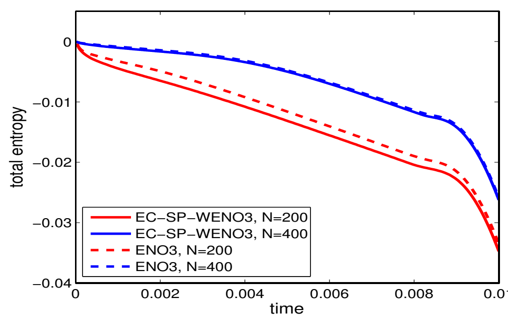

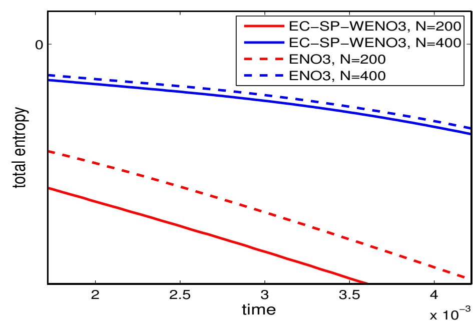

Figure 8: Example 2 (Greenshields model, $N = 2$): (left) relative change in total entropy of numerical solutions on two different mesh sizes, (right) enlarged view.

[7] J.S. Drake, J.L. Schofer, and A.D. May, *A statistical analysis of speed-density hypothesis*, Highway Res. Rec., 154 (1967), pp. 53–87.

[8] U.S. Fjordholm, S. Mishra, and E. Tadmor, *Arbitrary high-order essentially non-oscillatory entropy stable schemes for systems of conservation laws*, SIAM J. Numer. Anal., 50 (2012), pp. 544–573.

[9] U.S. Fjordholm, S. Mishra, and E. Tadmor, *ENO reconstruction and ENO interpolation are stable*, *Found. Comput. Math.*, 13 (2013), pp. 139–159.

[10] U.S. Fjordholm, S. Mishra, and E. Tadmor, *Energy preserving and energy stable schemes for the shallow water equations*. In F. Cucker, A. Pinkus, and M. Todd (Eds.), *Foundations of Computational Mathematics* Proceedings of FoCM held in Hong Kong, 2008. London Math. Soc. Lecture Notes Ser. 363, pp. 93–139. Cambridge University Press, 2009.

[11] U.S. Fjordholm and D. Ray, *A sign preserving WENO reconstruction method*, J. Sci. Comput., 68 (2016), pp. 42–63.

[12] M. Garavello, K. Han, and B. Piccoli, *Models for Vehicular Traffic on Networks*, American Institute of Mathematical Sciences, Springfield, MO, 2016.

[13] S. Gottlieb, C.-W. Shu, and E. Tadmor, *Strong stability-preserving high-order time discretization methods*, SIAM Rev., 43 (2001), pp. 89–112.

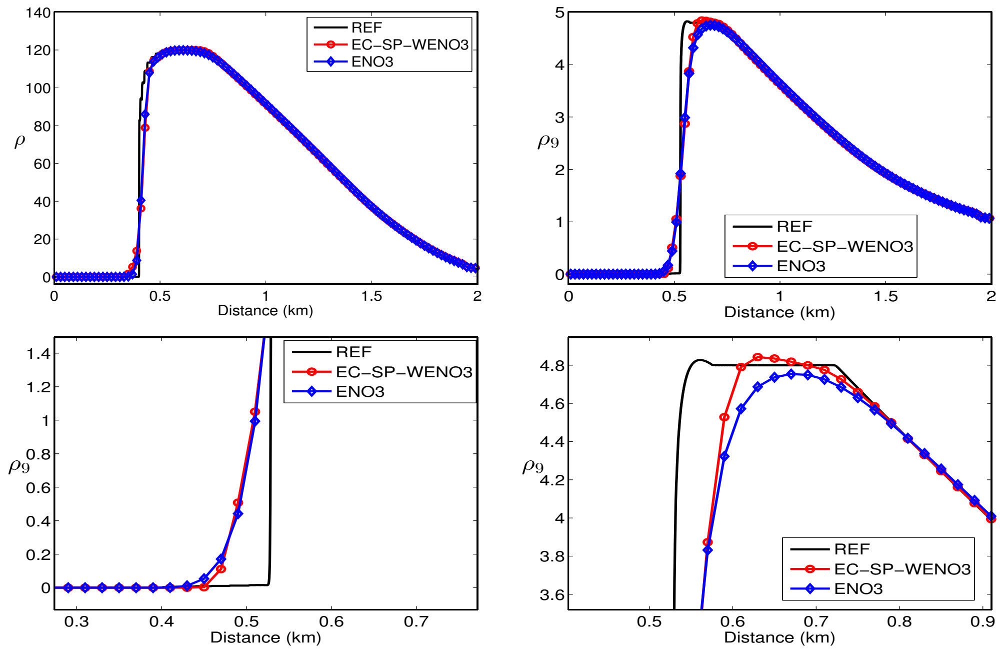

Figure 9: Example 3 (Greenshields model, $N = 9$): approximate solutions at $T = 0.01\,\mathrm{h}$ with $M = 100$ corresponding to (top left) the total density, (top right) class 9, (bottom) enlarged views.

[14] B.D. Greenshields, *A study of highway capacity*, Proc. Highway Res. Record, Washington, 14 (1935), pp. 448–477.

[15] F. Ismail and P.L. Roe, *Affordable, entropy-consistent Euler flux functions II: Entropy production at shocks*, J. Comput. Phys., 228 (2009), pp. 5410–5436.

[16] S. Jerez and C. Parés, *Entropy stable schemes for degenerate convection-diffusion equations*, SIAM J. Numer. Anal., 55 (2017), pp. 240–264.

[17] P.G. LeFloch, J.M. Mercier, and C. Rohde, *Fully discrete entropy conservative schemes of arbitrary order*, SIAM J. Numer. Anal., 40 (2002), pp. 1968–1992.

[18] M.J. Lighthill and G.B. Whitham, *On kinematic waves: II. A theory of traffic flow on long crowded roads*, Proc. Royal Soc. A, 229 (1955), pp. 317–345.

[19] D. Ray, *Third- Order Entropy Stable Scheme for the Compressible Euler Equations*, C. Klingenberg and M. Westdickenberg (eds.) Theory, Numerics and Applications of Hyperbolic Problems II, Springer Proceedings in Mathematics and Statistics 237, pp. 503–515.

[20] P.I. Richards, *Shock waves on the highway*, Oper. Res., 4 (1956), pp. 42–51.

[21] E. Tadmor, *Numerical viscosity and entropy conditions for conservative difference schemes*, Math. Comp., 43 (1984), pp. 369–381.

[22] E. Tadmor, *The numerical viscosity of entropy stable schemes for systems of conservation laws, I*, Math. Comp., 49 (1987), pp. 91–103.

[23] E. Tadmor, *Entropy stability theory for difference approximations of nonlinear conservation laws and related time-dependent problems*, Acta Numerica, 12 (2003), pp. 451–512.

[24] E. Tadmor and W. Zhong, *Entropy stable approximations of Navier-Stokes equations with no artificial numerical viscosity*, J. Hyperbolic Differ. Equ., 3 (2006), pp. 529–559.

[25] E. Tadmor and W. Zhong, *Energy preserving and stable approximation for the two-dimensional shallow water equations*, in *Mathematics and Computation: A Contemporary View*, Proceedings of the Third Abel symposium, Ålesund, Norway. Springer, 2008, pp. 67–94.

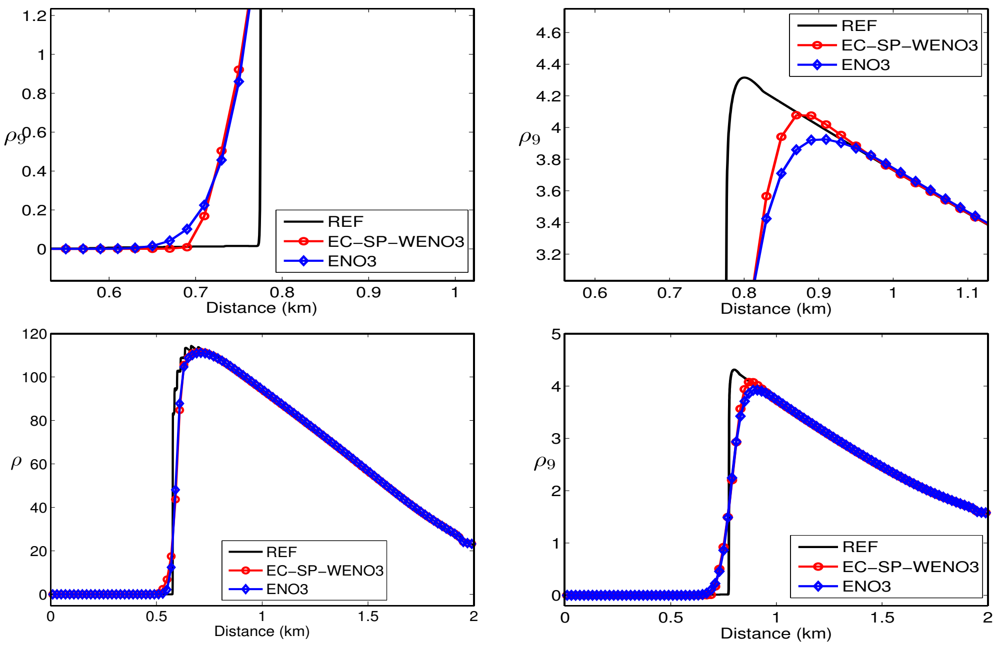

Figure 10: Example 3 (Greenshields model, $N = 9$): approximate solutions at $T = 0.015\,\mathrm{h}$ with $M = 100$ corresponding to (top left) the total density, (top right) class 9, (bottom) enlarged views.

[26] M. Treiber and A. Kesting, *Traffic Flow Dynamics*, Springer, Heidelberg, 2013.

[27] F. van Wageningen-Kessels, H. van Lint, K. Vuik, and S. Hoogendorn, *Genealogy of traffic flow models*, Euro J. Transp. Logist., 4 (2015), pp. 445–473.

[28] G.C.K. Wong and S.-C. Wong, *A multi-class traffic flow model—an extension of LWR model with heterogeneous drivers*, Transp. Res. A, 36 (2002), pp. 827–841.

[29] M. Zhang, C.-W. Shu, G.C.K. Wong, and S.C. Wong, *A weighted essentially non-oscillatory numerical scheme for a multi-class Lighthill-Whitham-Richards traffic flow model*, J. Comput. Phys., 191 (2003), pp. 639–659.

	$T = 0.01\,\mathrm{h}$				$T = 0.015\,\mathrm{h}$			
	EC-SP-WENO3		ENO3		EC-SP-WENO3		ENO3	
M	e_{tot}	Rate	e_{tot}	Rate	e_{tot}	Rate	e_{tot}	Rate
100	3.021	—	2.709	—	2.841	—	2.572	—
200	1.353	1.158	1.199	1.176	1.299	1.128	1.146	1.166
400	0.694	0.963	0.601	0.994	0.665	0.967	0.591	0.955
800	0.343	1.015	0.327	0.879	0.334	0.993	0.322	0.874
1600	0.173	0.987	0.170	0.939	0.168	0.987	0.175	0.877

Table 3: Example 3 (Greenshields model, $N = 9$): approximate total L^1-errors and convergence rates.

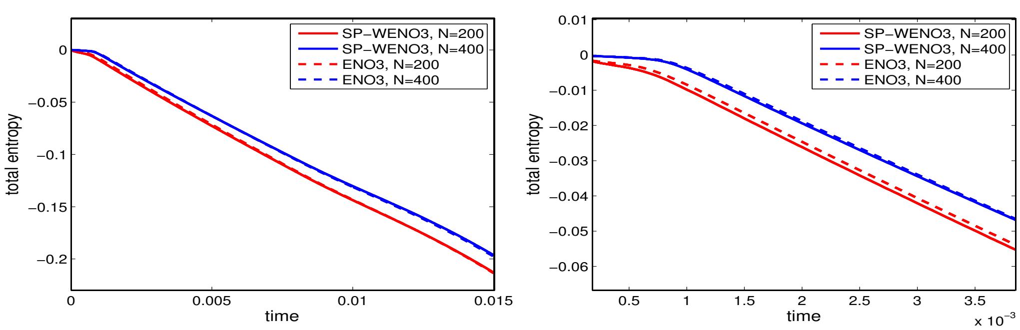

Figure 11: Example 3 (Greenshields model, $N = 9$): (left) relative change in total entropy of numerical solutions on two different mesh sizes, (right) enlarged view.

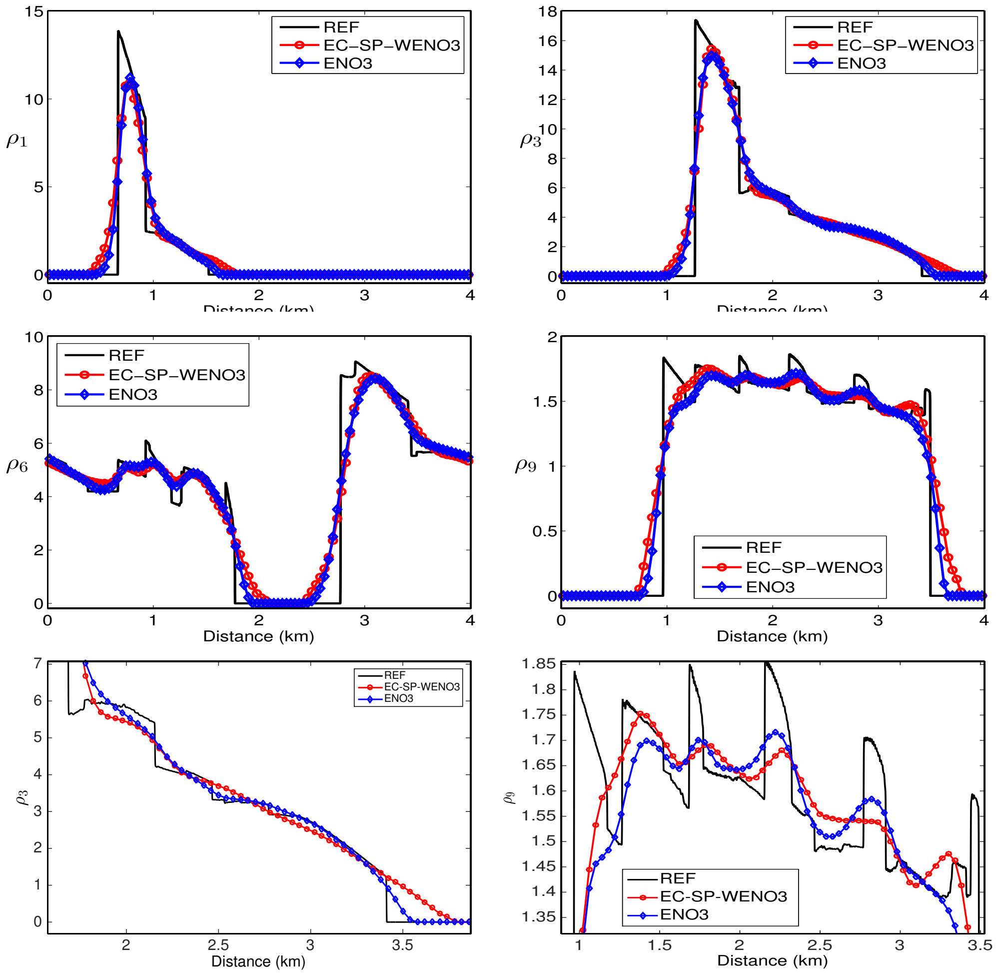

Figure 12: Example 4 (Greenshields model, $N = 9$, periodic boundary conditions): approximate solutions at $T = 0.1\,\mathrm{h}$ with $M = 100$ spatial cells corresponding to (top left) class 1, (top right) class 3, (middle left) class 6, (middle right) class 9, (bottom) enlarged views.

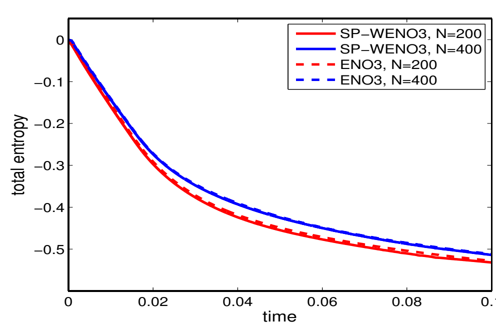

Figure 13: Example 4 (Greenshields model, $N = 9$, periodic boundary conditions): relative change in total entropy of numerical solutions on two different mesh sizes.

Centro de Investigación en Ingeniería Matemática (CI^2MA)

PRE-PUBLICACIONES 2018

2018-27 Ricardo Oyarzúa, Manuel Solano, Paulo Zuñiga: *A high order mixed-FEM for diffusion problems on curved domains*

2018-28 Gabriel Carcamo, Stephanie Caro, Fabián Flores-Bazán: *Extensions of the standard quadratic optimization problem: strong duality, optimality, hidden convexity and S-lemma*

2018-29 Javier A. Almonacid, Hugo S. Díaz, Gabriel N. Gatica, Antonio Marquez: *A fully-mixed finite element method for the coupling of the Stokes and Darcy-Forchheimer problems*

2018-30 Raimund Bürger, Paul E. Méndez, Ricardo Ruiz-Baier: *On H(div)-conforming methods for double-diffusion equations in porous media*

2018-31 Rodolfo Araya, Rodolfo Rodríguez, Pablo Venegas: *Numerical analysis of a time-domain elastoacoustic problem*

2018-32 Sarvesh Kumar, Ricardo Oyarzúa, Ricardo Ruiz-Baier, Ruchi Sandilya: *Conservative discontinuous finite volume and mixed schemes for a new four-field formulation in poroelasticity*

2018-33 Gabriel N. Gatica, Salim Meddahi: *On the coupling of VEM and BEM in two and three dimensions*

2018-34 Javier A. Almonacid, Gabriel N. Gatica: *A fully-mixed finite element method for the n-dimensional Boussinesq problem with temperature-dependent parameters*

2018-35 Lourenco Beirao-Da-Veiga, David Mora, Giuseppe Vacca: *The Stokes complex for virtual elements with application to Navier-Stokes flows*

2018-36 Marcelo Cavalcanti, Wellington Correa, Mauricio Sepúlveda, Rodrigo Véjar: *Well-posedness, exponential decay estimate and numerical results for the high order nonlinear Schrödinger equation with localized dissipation*

2018-37 Antonio Baeza, Raimund Bürger, Pep Mulet, David Zorío: *On the efficient computation of smoothness indicators for a class of WENO reconstructions*

2018-38 Raimund Bürger, Hector Torres, Carlos A. Vega: *An entropy stable scheme for the multiclass Lighthill-Whitham-Richards traffic model*

Para obtener copias de las Pre-Publicaciones, escribir o llamar a: Director, Centro de Investigación en Ingeniería Matemática, Universidad de Concepción, Casilla 160-C, Concepción, Chile, Tel.: 41-2661324, o bien, visitar la página web del centro: http://www.ci2ma.udec.cl




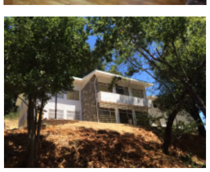

Centro de Investigación en Ingeniería Matemática (CI^{2}MA)

Universidad de Concepción

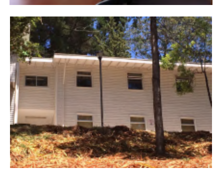
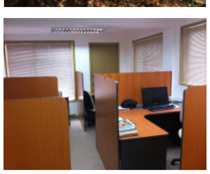

Casilla 160-C, Concepción, Chile

Tel.: 56-41-2661324/2661554/2661316

http://www.ci2ma.udec.cl